Nonlinear dynamics of a laser containing a modulated saturable absorber

Didier Dangoisse, Pierre Glorieux, and Daniel Hennequin
Laboratoire de Spectroscopie Hertzienne, Université de Lille I, F-59655 Villeneuve d'Ascq CEDEX, France
(Received 2 June 1989; revised manuscript received 5 January 1990)

In this paper, we report on the effect of an external force on the dynamical behavior of the CO_2 laser with a saturable absorber. Different regimes have been obtained as the modulation amplitude or frequency is changed. These regimes are compared to the standard phenomenology of the circle map, i.e., the transition from quasiperiodicity to locked regimes and chaos according to the Farey hierarchy with Arnold tongues. Return maps of the trajectories reconstructed from time series are shown. These results are compared with those of numerical simulations based on a simple model of the laser with a saturable absorber.

I. INTRODUCTION

The laser containing a saturable absorber (LSA) is an excellent illustration of the impact of nonlinear dynamics in the field of laser instabilities. In fact, the concepts currently in use in this field have recently proved very useful to understand and classify the different kinds of instabilities displayed by this system and are known collectively as passive Q switching (PQS).[1-11] In the CO_2 laser containing various absorbers such as SF_6, CH_3I, HCOOH, etc., different dynamical regimes occur. Depending on the operating conditions, one can observe limit cycles originating from a supercritical Hopf bifurcation or more complicated Shil'nikov-type dynamics involving an unstable saddle focus. Both regimes may evolve towards chaos as the parameters are changed.[6]

A major problem encountered by experimentalists who wish to use this system to generate high-peak-power pulses is the jitter that affects the pulses. In order to stabilize the frequency of the PQS pulses, a modulation may be applied to some control parameter of the LSA.[12] In this paper, we report on the effect of such a modulation on the dynamical behavior of the LSA. A similar problem was recently considered theoretically by Lauterborn and Eick, who made numerical simulations on a two-level model of a LSA with modulated pump[13] that could describe the experiments with modulated $Al_xGa_{1-x}As$-GaAs lasers.[14] The CO_2 laser containing a saturable absorber usually does not follow very well the predictions of two-level models, and experiments on a CO_2 laser with modulated saturable absorber (LMSA) must be performed in order to check its dynamical behavior. The various regimes obtained as the modulation amplitude or frequency is changed follow the standard phenomenology of periodically forced systems, i.e., the transition from quasiperiodicity to locked regimes according to the Farey hierarchy with Arnold tongues.[15] We have also paid attention to the fine structure of the locked regions in which period-doubling cascades have been observed.

This paper is organized as follows: in Sec. II, the experiment is presented and we discuss how the modulation acts on the LSA parameters. In Sec. III, a general outline of the experimental results is given. A more detailed study is given in the case of a LSA operating in the self-pulsing regime just below the first period-doubling bifurcation. The behavior of the system is discussed through the analysis of Poincaré sections of the phase-space trajectories reconstructed from time series. Section V is devoted to the comparison of these results with those of numerical simulations based on a simple model of the LSA.

II. MODULATION TECHNIQUE

The experiments were carried out on the same laser as that used in our previous investigations of the LSA dynamics.[6] The LSA is operated on the $P(32)$ CO_2 laser line at 10.7 μm (noted $10P32$ in the following) with CH_3I as a saturable absorber. This system was chosen since its different instabilities are well known and CH_3I was preferred to SF_6 since it has a permanent electric dipole. This property allows us to use the Stark effect to modulate sinusoidally the absorber. This technique makes possible an easy modulation of a laser parameter up to 200 kHz, i.e., well within the frequency range of the instabilities that appear in the CO_2+CH_3I LSA. Unfortunately, the bandwidth limitation of the amplifier used in the experiments and the capacitive character of the load induce a decrease of the modulation amplitude at high frequencies. The associated change of the driving amplitude as the frequency is swept was not compensated for in large frequency scans but was included in the results presented later.

The relation between the Stark field and the parameters of the absorber cannot be evaluated precisely. Indeed, the effect of a "static" electric field is to shift the energy levels in the absorber and as a consequence to change the detuning between the laser and the absorption frequencies. In CH_3I, the situation is much more complicated by the fact that many lines due to nuclear quadrupole coupling fall within the $10P32$ laser mode and are likely to interact with the laser radiation.[16] These lines are characterized by relatively large rotation quantum numbers resulting in a strong degeneracy of the energy levels and splitting in many M components of the absorp-

 ©1990 The American Physical Society

tion lines in the presence of the Stark field. Moreover, as the Stark field is highly inhomogeneous in our absorbing cell and the absorbing medium is Doppler broadened, one may consider that it essentially produces a modulation of the number of absorbing molecules, neglecting all detunings that are largely averaged out. For the results presented below, the amplitude of the modulation is estimated to be of the order of magnitude of 1% for a Stark voltage of 300 V.

III. GENERAL OUTLINE OF THE RESULTS

The CO_2 LSA exhibits several types of self-pulsing operations, classified in two principal groups that differ both by the pulse shapes and by their evolution as the control parameters are changed: (i) Type-I PQS is characterized by pulse shapes consisting of a high narrow peak followed by a series of n exponentially diverging undulations. We will denote this regime hereafter $P^{(n)}$, ν_{I} its associated repetition frequency, and $\nu_{\mathrm{II}}=T^{-1}$ the frequency of the fast undulation inside the pulse. As the experimental parameters are changed, this $P^{(n)}$ regime either evolves to the $P^{(n+1)}$ regime or doubles in period. (ii) In type-II PQS, the continuous-wave (cw) regime destabilizes through a supercritical Hopf bifurcation, i.e., starting with a small-amplitude limit cycle of period T similar to that of the undulations of the type-I PQS. As the parameters are changed, the amplitude of this cycle increases, and eventually, the regime can evolve to chaos through a period-doubling cascade.[6,8] Although hysteresis was observed between them, there is often a continuous transition between type-I and type-II PQS that actually represents limit cases, and there are many situations in which the dynamical regime of the LSA is intermediate between these regimes. It must be noticed that the two frequencies ν_{I} and ν_{II} evolve with the parameters of the system, and are locked together in the vicinity of the transition between type-I and type-II PQS.

The modulation-induced effects depend mainly on the free regime of the LSA, i.e., whether the LSA is operating in type-I or type-II PQS in the absence of external driving. In our experiments, conditions have been set so that the LSA is unstable and undergoes type-I or type-II PQS as the absorber pressure and/or the cavity detuning are changed. Figure 1 displays the phase diagram of our LSA versus these two parameters. Type-II PQS is indicated by T while $P^{(0)}$ corresponds to the type-I regime in which the laser emits single-peaked pulses. The transition from the T to the $P^{(0)}$ regime occurs in a continuous way in the region of the dashed line. In the hatched zone, the regime is either $P^{(1)}$ or $2T$, and the transition between these two regimes is also continuous. On the other hand, the period-doubling transition as well as the $P^{(0)}$-$P^{(1)}$ transition is abrupt.

Periodic forcing of the LSA has been performed in stable (cw) and different unstable regimes as follows.

(a) By periodically forcing the LSA working in the $2T$-$P^{(1)}$ *regimes,* or in another regime located in a region close to the bifurcation to these regimes, it has been possible to observe quasiperiodic and phase-locked regimes following the Farey hierarchy. The quasiperiodic regimes are due to the interaction of the external mode with frequency ν_m with an internal mode whose frequency ν_{II} is that of the type-II PQS. The ratio of the response frequency ν_r of the system to the modulation frequency is called the winding number; the regions of locked regimes are associated to a rational winding number, and are interpreted as the widest Arnold's tongues

$$\frac{\nu_r}{\nu_m}=\frac{p}{q},$$

where p and q are integers and q less than 6. The regimes of higher q correspond to narrower regions and so are difficult to analyze because of the blurring due to unavoidable technical noise.

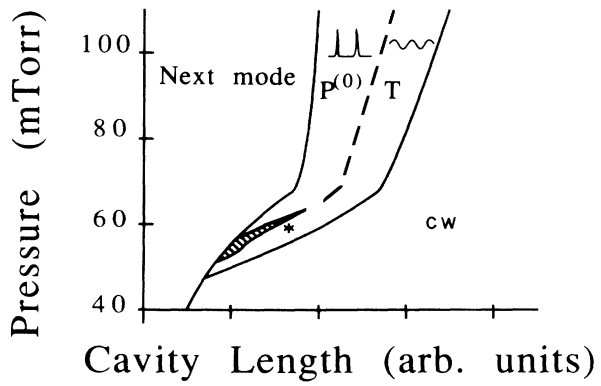

FIG. 1. Experimental phase diagram of the CO_2 laser with CH_3I as a saturable absorber. The laser operates on the $10P32$ with a discharge current of 15 mA through a mixture of CO_2, N_2, and He with respective partial pressure of 3 Torr, 5 Torr, and 8.5 Torr. The hatched zone on the figure corresponds to $2T$-$P^{(1)}$ regimes. The solid lines indicate abrupt transitions while the dashed one corresponds to a continuous change from type-I to type-II PQS. The region denoted "next mode" refers to the next longitudinal mode.

(b) The behavior described above also appears when the free LSA works in a type-II PQS regime far from the T-$2T$ bifurcation or in a cw regime close to the Hopf bifurcation. As the distance between the operating and the T-$2T$ bifurcation points is growing, the locking regions become narrower and finally only the principal one corresponding to $p=q=1$ remains visible at the experimental resolution. In this situation, a small-amplitude modulation at a frequency close to the internal one just induces a spectral narrowing, corresponding to a decreasing of the natural fluctuations of the system. The Hopf bifurcation does not constitute a limit for this behavior: in cw mode, the output of the forced system is periodic at the period of the external driving and its response exhibits a very flat resonance at a frequency close to that extrapolated from the values of those of the type-II PQS.[17] In all the cases, as the amplitude of the modulation is increased, the response exhibits a period-doubling cascade whose threshold increases as the system is operated farther from the T-$2T$ bifurcation region. Finally, the cascade disappears: this is certainly a consequence of the fact that in our experiments, the Stark modulation is not very efficient, and so the modulation of the absorption param-

eter remains small ($<10^{-2}$). However, even in the absence of period doubling, the shape of the signal evolves as a function of the position of the operating point in the phase diagram.

(c) Forcing the $P^{(0)}$ PQS far from the $P^{(1)}$-$2T$ transition, and more generally a $P^{(n)}$ PQS far from a transition from type-I to type-II PQS, induces a frequency locking with a sharp resonance at the fundamental frequency and a spectral narrowing of the laser intensity spectrum.

Note that the modulation effect on the cw mode below the Hopf bifurcation may be interpreted as a precursor of the bifurcation as locked regimes with Arnold tongues may be observed even on the nonpulsing LSA in the parameter region close to the onset of the PQS regime. Similar precursor effects were also observed in the other dynamical regimes as discussed in Sec. IV.

IV. DRIVING A LSA PULSE CLOSE TO THE T-$2T$ BIFURCATION

A detailed analysis of the behavior of the LMSA in the T-$2T$ bifurcation region is given here. More precisely, we will consider that all the parameters of the LSA are fixed so that the regime is T-periodic but close to the T-$2T$ bifurcation. In this case, the only significant free control parameters of the LMSA are the frequency and the amplitude of modulation. The basic structure of the two-dimensional reduced phase diagram remains similar to the Farey tree. However, many differences appear with the standard Farey hierarchy, as, e.g., the one obtained by the circle map $\theta_{n+1}=\theta_n+\Omega+(K/2\pi)\sin(2\pi\theta_n)$, where θ_{n+1} and θ_n are defined modulo 1 and Ω and K are parameters.[18] These differences may be classified in three groups concerning: (i) the macrostructure of the phase diagram, i.e., the global order of the regions of locking inside the regions of unlocked regime; (ii) the fine structure inside the tongues; and (iii) the fine structure of the unlocked regimes. Although these three regions of the parameter space are not completely independent, we will consider each one successively for the sake of clarity.

A. Macrostructure of the phase diagram

The Farey tree of the circle map is composed of an infinity of tongues that all intersect at the same value of the control parameter $K=K_d=1$. At K_d, the response of the system is always periodic, whatever the forcing frequency: the effective frequency of the response versus the frequency forcing follows the "devil's staircase." For a modulation amplitude larger than K_d, the system is chaotic in the regions where the tongues overlap; in the center of the tongues, it exhibits period-doubling bifurcations culminating in chaos. If we look at the response of the system to the forcing versus the modulation rate, the regime is first quasiperiodic at weak rates, then becomes periodic when the amplitude increases, and finally chaotic after an eventual period-doubling sequence. This scenario has already been observed in experiments on the Rayleigh-Bénard system.[19]

In order to determine the global structure of the phase diagram of the LMSA reduced to the two above-mentioned significant dimensions, different alternatives are possible: the simplest ones consist of exploring the parameter space along one of the main directions, i.e., varying one of the parameters while the other one is fixed, and repeating this operation for different values of the fixed parameter. Using the same periodic sampling technique as in our study of the laser with modulated loss and/or frequency,[20] i.e., a sample-and-hold module triggered by the external modulation, the real-time evolution of the LMSA bifurcation diagrams is monitored as a function of the control parameter. As an example, Fig. 2 shows the sampler output when the frequency ν_m of the driving field is swept in the 20–200 kHz range. When the modulated laser is working in a periodic regime, the pulsing frequency is locked to that of the external field at a value given by $\nu_{II}/p=\nu_m/q$, where p and q identify the tongue. Thus the sampler triggered by the external driving delivers q different output values. On the other hand, when the system is quasiperiodic or chaotic, the output covers a large range of values. This technique does not permit us to distinguish between quasiperiodic and chaotic regimes. Note also that owing to the amplifier saturation, the effective modulation rate is not constant in Fig. 2, but decreases as a function of the frequency. This is taken into account in the following presentation of the results.

The phase diagram obtained by this method put in evidence an original behavior at large modulation rate. When two tongues coalesce, the one corresponding to the higher q disappears for the benefit of the other one. As a consequence, the response of the system at increasing modulation rate, but fixed frequency, may eventually reach different successive regimes: it is first quasiperiodic, then may be periodic when crossing the border of a tongue. Several successive changes in the period may occur as the system jumps to "stronger" tongues. Unfortunately, the present status of our setup does not allow us

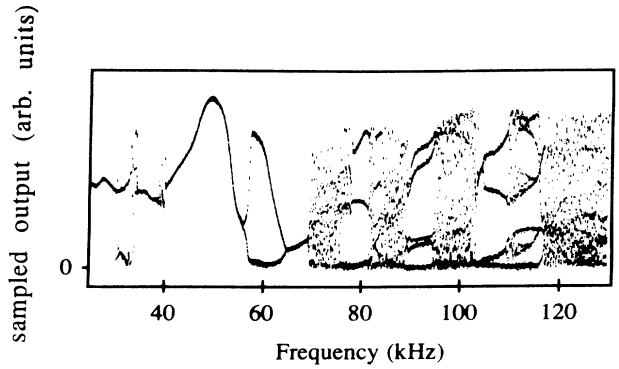

FIG. 2. Bifurcation diagram of the LSA in the presence of external driving for a LSA operated in a type-II regime close to the T-$2T$ bifurcation as indicated by the star in Fig. 1. The sampled output of the laser is displayed vs the driving frequency. The natural instability frequency of the laser is 57 kHz. Because of the bandwidth limitation of the amplifier used to do this record, the amplitude of modulation is 500 V at 30 kHz and decreases continuously to reach 80 V at 130 kHz.

to verify if this behavior keeps on for higher q tongues, and so for lower modulation rates. For this reason no attempt was made to find a critical line in this system. Moreover, such a critical line may have a complicated shape in real systems and then loses most of its significance in such cases.

B. Fine structure of the tongues

For a weak force, the regime of the LMSA in a locked region is periodic at the frequency $\nu_{II}/p=\nu_m/q$. The sampling technique permits us to determine easily the value of q. The p number can then be deduced from the value of the eigenfrequency ν_{II}. However, p and q do not completely describe the signal. In particular, two signals with the same period may present a completely different shape. In this case, the only way to separate them is a phase-space plot. This is beyond the scope of this paper in which we studied the global evolution of the response in the different regions of the parameter space.

When the rate of forcing increases, a qualitative change in the response of the system occurs, consisting in the presence of period-doubling bifurcations followed by some irregular regimes that are likely to be chaotic since they appear after a period-doubling cascade. After, e.g., the first period-doubling bifurcation, the response frequency of the system evolves from $\nu_{II}/p=\nu_m/q$ to $\nu_{II}/2p=\nu_m/2q$ and is then identified by $2q$ branches in the bifurcation diagram. More generally, the frequency of the system in the period-doubling cascade is given by $\nu_{II}/2^n p=\nu_m/2^n q$, where n is an integer. After the cascade, the regime loses its regularity and the experimental diagram resembles a continuous like set of points. This is illustrated in Fig. 2, in the case where the free laser is operated in a periodic type-II PQS regime at about 57 kHz, just at the edge of the period-doubling region as shown in Fig. 1. As the external frequency is swept, various locking regions are observed, for instance, around 57 kHz ($p/q=1$), 82 kHz ($p/q=2/3$), 95 kHz ($p/q=3/5$), and 115 kHz ($p/q=1/2$). Between these main locking regions, narrower ones can also be observed but the most prominent feature is the fine structure which appears inside the locking regions. In the $p/q=1/2$ tongue, the effective response of the laser depends on the position inside the tongue: for example, at $\nu_m=107$ kHz, the actual response is at 53.5 kHz, i.e., around ν_{II} (but slightly different from that value because of the locking on the modulation frequency). In contrast, at $\nu_m=111$ or 121 kHz, the response frequency is $\nu_m/4$, i.e., about $\nu_{II}/2$. At $\nu_m=119$ kHz, eight branches appear in the bifurcation diagram, so the response frequency is $\nu_m/8\cong\nu_{II}/4$. One can see also a response at $\nu_m/16$ at 116 kHz and an erratic one at 114 kHz. This last regime is expected to be chaotic since it occurs after a period-doubling cascade, and can be described as "locked" since it appears inside a region of locking. Note also that the sampled values are spread over the same range of values as during the corresponding period-doubling cascade; this means that we observe here the first steps of the inverse cascade.

Figure 3 gives the Farey tree for a set of parameters

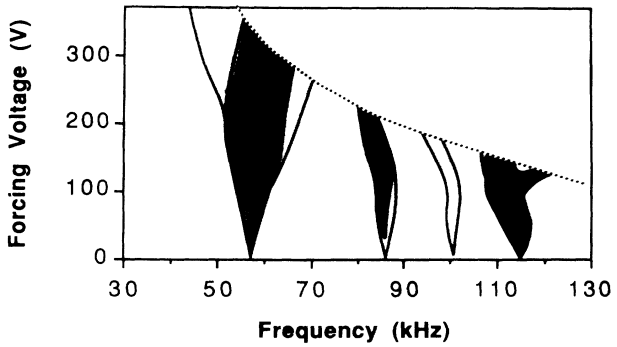

FIG. 3. Evolution of the dynamical regimes of the periodically driven LSA as a function of the frequency and the amplitude of the external driving. The free LSA was operating in the conditions of the star in Fig. 1. In these conditions, the efficiency of the modulation and the amplifier saturation did not allow the modulation rate to increase enough to observe the intersection between the tongues. The white regions correspond to nonperiodic regimes, which may be either chaotic or quasiperiodic. The shaded zones correspond to locked regimes. In the bright gray region, the period of the driven system is the same as that of the forcing one. The middle (dark) gray corresponds to a period doubling (period quadrupling) of the response compared to the forcing. The white zone over the dotted line corresponds to a region that could not be explored because of the bandwidth limitation of the amplifier used in this experiment.

where it was not technically possible to increase the modulation amplitude enough to observe the collision between the different tongues. This figure has been constructed using the technique described above and corresponds to a series of bifurcation diagrams whose resolution was chosen to sweep the $p/q=1$ and the $p/q=1/2$ tongues. Consequently, only four tongues are visible, corresponding to the widest ones. Other tongues may be obtained when decreasing the sweeping amplitude. As mentioned above, the quasiperiodic regimes are not differentiated from the chaotic ones and are represented both in white in the phase diagram. On the contrary, the periodic regimes, easily identified, are reported in Fig. 3 in different gray intensities according to the $\nu^m/2^n q$ ratio: light for $n=0$, medium for $n=1$, and dark for $n=2$. The global structure inside the tongues appears clearly, showing a succession of period-doubling bifurcations. The threshold of appearance of these bifurcations is very low compared to the ones observed in other systems. This may be explained by the fact that for this set of parameters, the unmodulated LSA is close to bifurcating to a period-doubled regime. So the modulation acts in a way as a precursor of the bifurcation. Moreover, the comparison of the tongues shows differences in the cascade, principally in the position of the bifurcation points with respect to the vertical axis. For example, the period doubling appears much more rapidly in the $p/q=1/2$ tongue than in the $p/q=1$ tongue.

It must also be noticed that the period-doubling bifurcations do not appear symmetrically with respect to the center of the locking region and that their shape seems to indicate that there could be a dynamical effect induced by

the fast sweep of the control parameter.[21] However, it has been carefully checked that although a small delay of the bifurcations could occur in our experiments, most of the asymmetry is a genuine effect. This denotes the presence of an underlying asymmetry in the tongue, probably coming from the presence of the other eigenfrequency ν_I introduced in Sec. III.

The overall shape of the sampled signal in the locked regions with a rapid change around the subharmonics of the eigenfrequency is due to a rapid phase shift similar to that occurring in a resonant circuit driven near resonance.

C. Unlocked regimes

We have shown above that there exists a locked chaos inside the tongues on the basis of the period-doubling cascade leading to this regime. In the case of the circle map, the regime is quasiperiodic outside the locked region. In order to differentiate this quasiperiodic regime from a possibly chaotic one, the bifurcation diagram described above is no more sufficient. The spectrum of the signal can provide the information, although it is sometimes difficult to differentiate a quasiperiodic spectrum from a chaotic one as in the experiments, the frequency jitter broadens the peaks of the spectrum. The previous technique used to obtain the bifurcation diagrams has been modified to include a second sampling unit, and to give an oscilloscope display of the nth sampled value versus the $(n+1)$th one. In a phase space where the phase of the signal constitutes one of the directions, this plot represents a first return map of the attractor. Such plots are extremely powerful in assigning the dynamical behavior of an unstable system: a limit cycle is represented by a set of q points [see, e.g., Fig. 4(a)], a chaotic attractor by a noninversible curve, and a quasiperiodic torus by a closed curve. This technique allows us to check that for a weak amplitude modulation, the regime outside the tongues is quasiperiodic [Fig. 4(b)]. The first return map is a closed curve whose complexity depends on the neighboring regimes. For example, in the vicinity of a locked region, the curve presents points of higher probability that are the extension of the points of the return map of the locked region. This is the case of Fig. 4(b) which corresponds to a quasiperiodic regime close to the $p/q=4/9$ locking.

If the force is increased, windings appear in the closed curves representing the return map of the attractor [Fig. 4(c)]. This type of destruction of a two-dimensional torus that transforms directly into a chaotic attractor arises in the Curry and Yorke model. Illustrations of the behavior of this two-dimensional map may be found in Ref. 22, and a similar scenario has already been observed in some experimental systems, such as, e.g., Rayleigh-Bénard convection.[23] The chaotic regime associated with the "winding" attractor is sometimes called "chaotic phase intermittency." In the LMSA, the transition to such a chaotic regime outside the Arnold tongues seems to occur at very different modulation amplitudes when the frequency of the forcing is scanned, and this is another argument which confirms the complexity of the critical line.

If the force is increased further, there appear regions where the return map is neither a set of points nor a closed curve, but a more complicated pattern [Fig. 4(d)] composed of isolated surfaces. The complexity and the shape of these attractors differ clearly from those encountered in the usual scenario following the destruction of a two-dimensional torus, where the attractor remains as a "deformation" of the torus. On the contrary, the system seems here to evolve through a phase transition, increasing its complexity. The presence of the second eigenfrequency ν_I whose role was already suspected inside the tongues, may contribute to this evolution. In the experiments presented here, the quasiequality of ν_I and ν_{II} prevents a detailed analysis. Future investigations in another situation should allow clarification of this point.

V. NUMERICAL SIMULATIONS

It is interesting to compare these results with those provided by numerical simulations. This numerical work was realized on the basis of the modified three-level model that we used in the modeling of the dynamical behavior of the LSA.[24] This model, which assumes a fast absorber, provides a good qualitative agreement with the experimental results concerning the unmodulated CO_2 LSA. It is composed of a set of three nonlinear coupled differential equations:

$$\dot{I}=I(U-1)-\frac{I\bar{A}}{1+aI} ,$$

$$\dot{U}=\epsilon[W-U(1+I)] ,$$

$$\dot{W}=\epsilon(A+bU-W) ,$$

where I is the laser intensity, U is the scaled population inversion in the active medium with associated damping rate ϵ, and W is a variable representing the source term in the three-level model. In this fast absorber model, the passive cell only introduces intensity-dependent losses represented by a scaled absorption $\bar{A}$ and a relative saturability a. A is the laser gain, b depends on the ratio of relaxation parameters and is fixed hereafter at a value of 0.85 as in Ref. 24. Overdots refer to derivatives with respect to time in units of the cavity damping time.

The influence of the Stark modulation has been introduced by considering that the main effect of the electric field is to change the number of absorbing molecules as discussed in Sec. II. So, the equations of the LMSA are the same as those of the LSA, except for $\bar{A}$ that is now time dependent:

$$\bar{A}=\bar{A}_0[1+m\cos(2\pi\nu_m t)] ,$$

where m is the amplitude of the forcing and ν_m the modulation frequency.

In this model, the gain threshold of the LSA is given by $A=A_{th}\equiv(\bar{A}_0+1)(1-b)$. For $A>A_{th}$, this system has two fixed points: the first one corresponds to an intensity $I_0=0$; the second one corresponds to an intensity $I_+\neq 0$. The respective stability of these two points determines the dynamics of the LSA. These dynamics may also depend on the presence of other attractors as, e.g., limit cycles.

It is interesting to relate the chosen parameters to the dynamical behavior of the LSA in the absence of modulation and very different situations may occur since the Shil'nikov dynamics of the LSA give rise to a large variety of signals. In a first step, simulations have been undertaken in the type-II PQS region, which corresponds to the experimental situation and where the interpretation of the calculated results is likely to be easier. Using the same set of parameters as in Ref. 24, the situation is complicated by the existence of a large bistability between the type-II PQS and I_+ stable regime as A is chosen as a control parameter. So it appears difficult to modulate moderately the system without forcing it to fall into the basin of attraction of the I_+ stable point.

The parameters have been slightly modified with respect to Ref. 24, as indicated in Table I, in order to reduce the bistability domain and the values have been chosen so that the LSA in the absence of modulation works in the conditions indicated by the star in Fig. 1. Thus, all the other parameters being held constant, a change of the pressure in the absorber gives the evolution cw$\rightarrow T\rightarrow 2T$ or $P^{(1)}\rightarrow P^{(0)}$ with bifurcations at 36.5, 37.15, and 40 mTorr, respectively. The transition from $2T$ to $P^{(1)}$ is continuous. Such a scenario corresponds to the experimental one. However, as the modulation parameter is the absorption $\overline{A}$, it is interesting to look at the evolution of the system at constant pressure and varying $\overline{A}$. It appears that at a pressure of 37 mTorr, which corresponds to the situation of Sec. IV, the scenario as a function of $\overline{A}$ is cw$\rightarrow T\rightarrow 2T\rightarrow 4T$ continuous transition to $2P^{(1)}\rightarrow P^{(1)}\rightarrow P^{(0)}$ with bifurcation points in 1.825, 1.860, 1.900, 1.970, and 2.570, respectively. The operating point corresponding to the values of Table I is in $\overline{A}=1.850$ and is separated from the T-$2T$ bifurcation by $\Delta\overline{A}=0.01$. In the following, the modulation rates will be expressed in units of $\Delta\overline{A}$.

In the model, the response to an external driving of the LSA working far from the T-$2T$ bifurcation is characterized by narrow tongues without fine structures. Such a behavior is similar to that observed experimentally for

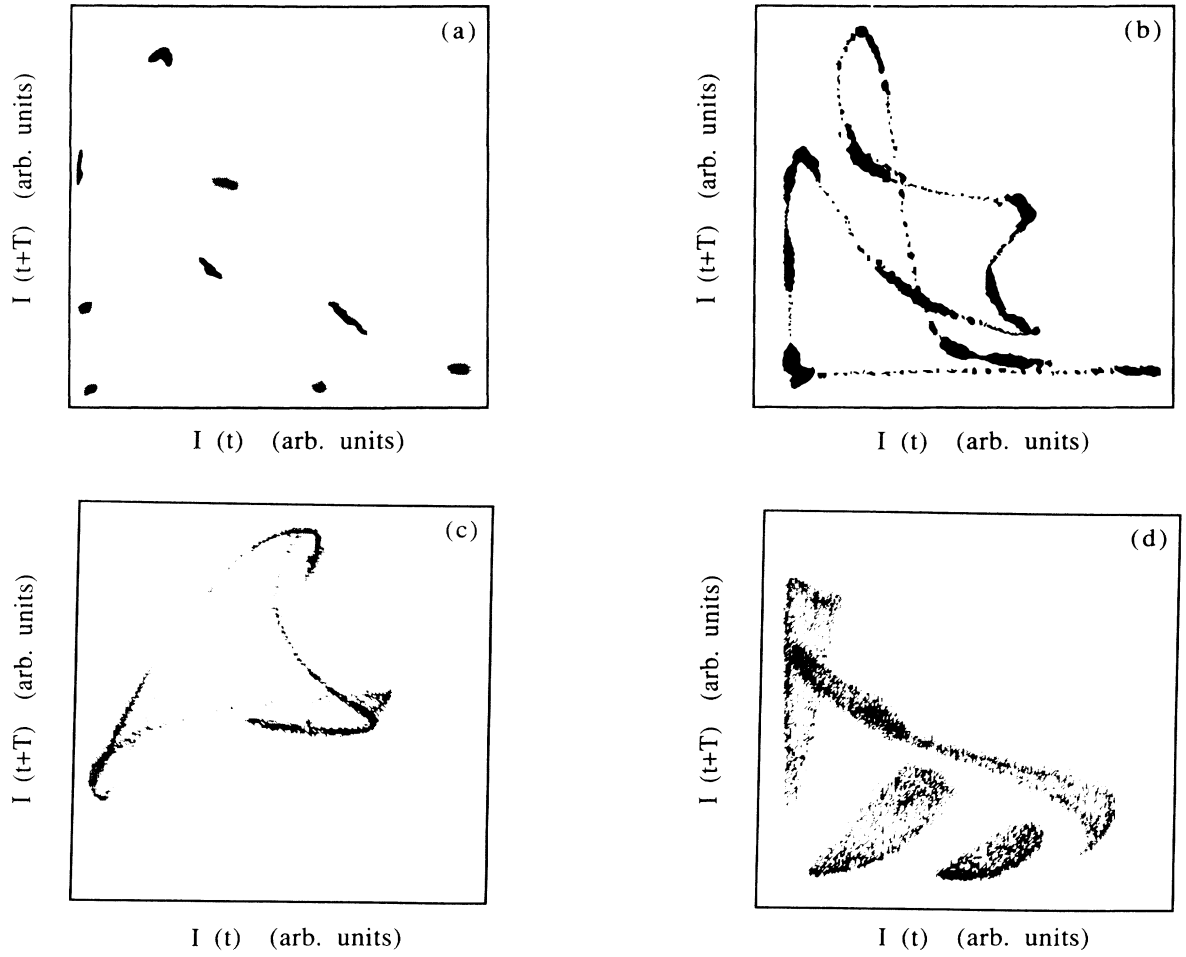

FIG. 4. Experimental return maps of the regimes of the LMSA $I(t+T)$ vs $I(t)$ where $T=\nu_m^{-1}$. The free LSA was operating in the same conditions as in Fig. 3 with the following forcing: (a) this periodic regime obtained for a modulation of 60 V at $\nu_m=129$ kHz corresponds to the winding number 4/9; (b) just nearby, at $\nu_m=135$ kHz with the same amplitude of modulation, the regime is quasi-periodic, some parts of the trajectory have a higher density of points; (c) chaos is obtained at $\nu_m=102$ kHz for 100 V of modulation; (d) chaos again at $\nu_m=147$ kHz and 40 V of modulation.

TABLE I. Values of the parameters used in the calculations. P denotes pressure in mTorr.

ϵ	0.137
A	2
$\overline{A}_0$	$0.05P$
a	$120/P$
b	0.85

the same type of situation.

A more detailed study has been done at 37 mTorr corresponding to the situation developed in Sec. IV. We follow the same scheme of analysis as in that section.

A. Macrostructure of the phase diagram

The differences between the global structure of the calculated phase diagram and the circle map are the same as in the experimental case. That concerns mainly the behavior of the system at the interaction between two tongues. Figure 5 shows a phase diagram resulting from the calculations with the set of parameters of Table I. For the sake of clarity, only the three first larger tongues have been represented, i.e., the ones associated with the winding numbers 1, 1/2, and 2/3. The 1/3 tongue is outside the limits of the figure. The free system oscillates at 53 kHz. The same convention as in Fig. 3 is applied for the representation of the different regimes. In particular, the quasiperiodic regimes and the chaotic ones have not been dissociated and are represented both in white. The behavior of the LMSA at high modulation rate is illustrated in this figure. It differs from that observed, e.g., in the logistic map, because the collision between two tongues results in the disappearance of one of the tongues for the benefit of the other one. For instance, in Fig. 5, for a modulation amplitude of $40.7\Delta\overline{A}$, the $p/q=2/3$ tongue collides with the $p/q=1$ tongue and the former disappears. Such a behavior has also been observed experimentally. However, the modulation rates appearing in Fig. 5 may seem high, and result from the deliberate choice of presenting the whole phenomenology of the model on a single set of parameters, corresponding to the experimental conditions of Fig. 3. The precise comparison of Figs. 3 and 5 shows that modulation amplitudes used in the simulations are typically five times larger than the ones estimated experimentally. This difference, which has to be softened owing to the poor quality of the estimation of the experimental modulation rates, could be reduced by a better choice of the parameters in the simulations.

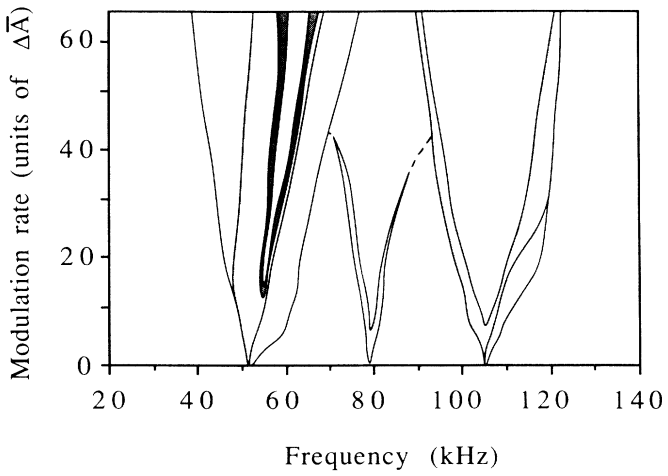

FIG. 5. Calculated phase diagram as a function of the driving frequency. The parameters used are those of Table I. The frequency of the free system is 53 kHz. For the sake of simplicity, only the three first main tongues have been represented: they are respectively associated with the winding numbers 1 (53 kHz), 1/2 (106 kHz), and 2/3 (89 kHz). The 1/3 tongue is outside the limits of the figure. The dashed lines of the 2/3 tongue have been represented to clarify the figure, but the corresponding limit has not been accurately checked. The white regions correspond to nonperiodic regimes, identified as chaos inside the tongues. On the contrary, outside the tongues, these regimes may be either chaotic or quasiperiodic. The colored zones correspond to locked regimes. In the bright gray region, the period of the driven system is the same as that of the forcing one. The middle (dark) gray corresponds to a period doubling (period quadrupling) of the response compared to the forcing. The other components of the period-doubling cascade are too narrow and so not represented here.

B. Fine structure of the tongues

The same type of structure as in the experiments reported above is found in the numerical simulations (Fig. 5). In the p/q tongues, a series of period-doubling cascades gives successively the regimes $(p/2^n q)\nu_m$. This cascade culminates in an aperiodic regime similar to the experimental one, and which may be identified as chaos. This chaos is characterized by a power spectrum with a continuous component and a maximum in ν_m, which corresponds to a "locked" situation. Figure 6(a) shows the return map of this regime. Such a return map is characteristic of a chaos following the Feigenbaum scenario. Similar diagrams were obtained in the case of a laser with modulated losses,[20] for the same type of situation. In fact, in the particular case where the modulation frequency is close to the eigenfrequency of the LSA, the LMSA is very similar to the laser with internal modulation (LIM). So it is not surprising to find a Feigenbaum scenario at low modulation amplitude, and a more detailed analysis of the numerical results should show the same variety of phenomena such as crises, periodic windows, etc., as was observed in the LIM.

The other characteristics of the experimental Farey tree (asymmetry, shift of the bifurcation points inside the different tongues) are also present here. Note that the chaotic region in the $p/q=1$ tongue is shifted to higher frequencies with increasing amplitudes. Such a shift was not observed experimentally, but this may be attributed to the poor resolution of the experiments in which the driving frequency is swept.

C. Unlocked regimes

Outside the tongues and for a weak forcing, the response in the model of the LSA is quasiperiodic. This

appears clearly in the spectrum of the signal, or in the first return map, as, e.g., in Fig. 6(b). This regime is obtained for a modulation amplitude of $5\Delta\overline{A}$ at a frequency of 119.25 kHz, corresponding to a winding number close to 9/4. On the curves nine zones of higher density are visible, corresponding to the nine points of the locked regime. Although the shape of this curve is not identical to that of Fig. 4(b), their gross features with accumulation points and trailing ends lying on a "close curve" look similar.

At a stronger force the same type of chaotic regime as in the experiments may occur. Because of the very complex distribution of the quasiperiodic and chaotic regimes in the phase diagram, they were not distinguished in Fig. 5. But a return map of a chaotic regime shows on Fig. 6(c) a remarkable analogy with Fig. 4(c) and with the maps obtained from the Curry and Yorke model.[22] This confirms the hypothesis of the destruction of the two-dimensional torus. A precise analysis shows that at the resolution of the calculations, the torus with an irrational winding number can transform directly in a chaotic attractor, without the intermediate locked region.

At increased modulation rates, the chaotic behavior becomes more complicated and the branches of the associated return map "broaden" [Fig. 6(d)], leading to the same type of pattern as in Fig. 4(d). The spectrum of such a signal presents a continuous component with a maximum at ν_{II}, leading to a kind of "free" chaos, since ν_{II} is the eigenfrequency of the free system. The transition between the two types of regimes is continuous, and so the second one appears as a transformed version of the first one. A more precise characterization of the attractor should be reached by a more detailed study of the attractor, as that provided by, e.g., a dimensionality analysis.

VI. CONCLUSION

We have shown that the basic structure of the response of the LSA to an absorption modulation corresponds to the Farey hierarchy. However, a detailed analysis of the behavior of the LMSA reveals some important differences that can be classified as follows: (i) the accumulation point of the tongues associated to a devil's staircase is ab-

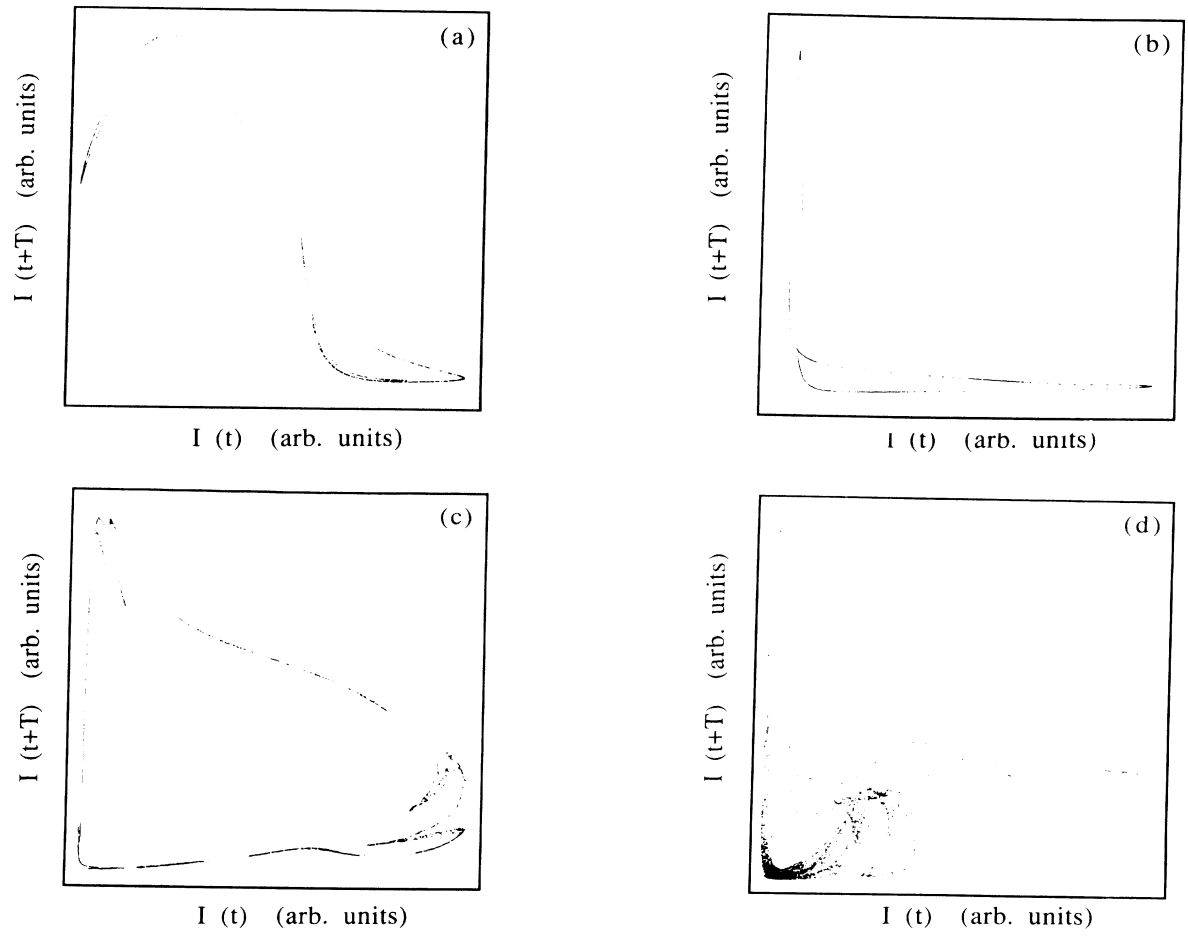

FIG. 6. Theoretical return maps of the regimes of the LMSA $I(t+T)$ vs $I(t)$, the parameters being those of Table I. The conditions of modulation and the associated temporal regimes are (a) $\nu_m = 61$ kHz, $m = 0.3 = 55\Delta\overline{A}$, "locked" chaos; (b) $\nu_m = 119.25$ kHz, $m = 0.0275 = 5\Delta\overline{A}$, quasiperiodic regime just at the edge of the locking at 4/9 ν_m; (c) $\nu_m = 70$ kHz, $m = 0.019 = 3.5\Delta\overline{A}$, "winding" chaos; (d) $\nu_m = 70$ kHz, $m = 0.075 = 14\Delta\overline{A}$, "free" chaos.

sent. In the LMSA, the collision between two tongues leads to the disparition of the "weaker" one (ii) a period-doubling cascade culminating in chaos occurs in the tongues at low modulation amplitude. (iii) Outside the tongues, a chaos coming from the destruction of the quasiperiodic torus is observed.

The addition of all these phenomena gives a tree which is much more complicated than the Farey tree of the circle map. For instance, increasing the modulation amplitude at constant frequency, it is possible to find successively quasiperiodicity, various periodic regimes, and different types of chaos ordered in a rather complicated way.

A simple model of the LMSA provides an excellent qualitative agreement with the experimental results.

Future investigations may concern quantitative characterizations of the observed regimes, such as dimensionality analyses, but the qualitative description of the behaviors of the LMSA should be completed. Indeed, several phenomena that have not been presented here have been observed in our experiments. In particular, this is the case for bistabilities between different regimes, and for the response when the LSA presents a more complex phase diagram, including, e.g., $P^{(n)}$, $n > 1$ regimes. In such conditions, the role of the second eigenfrequency of the LSA should be more clearly exhibited.

This paper reports only a preliminary investigation of the LMSA. The LSA displays a very large variety of dynamical behaviors and our study could be extended in different directions.

[1]A. Jacques and P. Glorieux, Opt. Commun. **40**, 455 (1982); E. Arimondo, F. Casagrande, L. Lugiato, and P. Glorieux, Appl. Phys. B **30**, 57 (1983).

[2]E. Arimondo, P. Bootz, P. Glorieux, and E. Menchi, J. Opt. Soc. Am. B **2**, 193 (1985).

[3]N. B. Abraham, P. Mandel, and L. M. Narducci, in *Progress in Optics,* edited by E. Wolf (North-Holland, Amsterdam, 1988), Vol. 25.

[4]T. Erneux, P. Mandel, and J. F. Magnan, Phys. Rev. A **29**, 2690 (1984); P. Mandel and T. Erneux, *ibid.* **30**, 1893 (1984); T. Erneux and P. Mandel, *ibid.* **30**, 1902 (1984).

[5]P. Glorieux, J. Phys. (Paris) **67**, 433 (1987).

[6]D. Dangoisse, A. Bekkali, F. Papoff and P. Glorieux, in *Proceedings of the International Workshop on Instabilities and Chaos in Nonlinear Optical Systems,* edited by N. B. Abraham, E. Arimondo, and R. Boyd (Editrice, Pisa, 1987); Europhys. Lett. **6**, 335 (1988).

[7]E. Arimondo, C. Gabbanini, E. Menchi, D. Dangoisse, and P. Glorieux, in *Optical Instabilities,* Vol. 4 of *Cambridge Studies in Modern Optics,* edited by R. W. Boyd, M. G. Raymer, and L. M. Narducci (Cambridge University Press, Cambridge, 1986).

[8]D. Hennequin, F. de Tomasi, B. Zambon, and E. Arimondo, Phys. Rev. A **37**, 2243 (1988); D. Hennequin, F. de Tomasi, L. Fronzoni, B. Zambon, and E. Arimondo, Opt. Commun. **70**, 253 (1989).

[9]F. de Tomasi, D. Hennequin, B. Zambon, and E. Arimondo, J. Opt. Soc. Am. B **6**, 45 (1989); E. Arimondo, D. Hennequin, and P. Glorieux, in *Noise in Nonlinear Dynamical Systems,* edited by F. Moss and P. V. E. McClintock (Cambridge University Press, Cambridge, 1989), Vol. 3.

[10]M. Tachikawa, F. Hong, K. Tanii, and T. Shimizu, Phys. Rev. Lett. **60**, 2266 (1988); M. Tachikawa, K. Tanii, M. Kajita, and T. Shimizu, Appl. Phys. B **39**, 83 (1986); K. Tanii, M. Tachikawa, M. Kajita, and T. Shimizu, J. Opt. Soc. Am. B **5**, 24 (1988); M. Tachikawa, K. Tanii, and T. Shimizu, *ibid.* **4**, 387 (1987).

[11]A. Bekkali, F. Papoff, D. Dangoisse, and P. Glorieux, J. Phys. (Paris) Colloq. **49**, C2-349 (1988).

[12]M. Ouhayoun (private communication).

[13]W. Lauterborn and I. Eick, J. Opt. Soc. Am. B **5**, 1089 (1988).

[14]H. G. Winful, Y. C. Chen, and J. M. Liu, Appl. Phys. Lett. **48**, 616 (1985).

[15]M. H. Jensen, P. Bak, and T. Bohr, Phys. Rev. Lett. **50**, 1637 (1983); J. Stavans, F. Heslot, and A. Libchaber, *ibid.* **55**, 596 (1985); J. Stavans, Phys. Rev. A **35**, 4314 (1987); S. Martin and W. Martienssen, Phys. Rev. Lett. **56**, 1522 (1986).

[16]E. Arimondo and P. Glorieux, Phys. Rev. A **19**, 1067 (1979).

[17]E. Arimondo and P. Glorieux, Appl. Phys. Lett. **33**, 49 (1978).

[18]For a recent review see J. M. Gambaudo and C. Tresser, in *Le Chaos,* edited by P. Bergé (Commissariat à l'Energie Atomique, Paris, 1989), Chap. III.

[19]J. A. Glazier, M. H. Jensen, A. Libchaber, and J. Stavans, Phys. Rev. A **34**, 1621 (1986).

[20]T. Midavaine, D. Dangoisse, and P. Glorieux, Phys. Rev. Lett. **55**, 1989 (1985); D. Dangoisse, P. Glorieux, and D. Hennequin, Phys. Rev. A **36**, 4775 (1987).

[21]R. Kapral and P. Mandel, Phys. Rev. A **32**, 1076 (1985); R. Mannela, F. Moss, and P. V. E. McClintock, Phys. Lett. A **144**, 68 (1986); C. Grebogi, E. Ott, and J. A. Yorke, Physica D **7**, 81 (1983); Phys. Rev. Lett. **57**, 1284 (1986); C. Grebogi, E. Ott, F. Romeiras and J. A. Yorke, Phys. Rev. A **36**, 5365 (1987); F. Papoff, D. Dangoisse, E. Poite-Hanoteau, and P. Glorieux, Opt. Commun. **67**, 358 (1988).

[22]J. Curry and J. A. Yorke, in *Structure of Attractors in Dynamical Systems,* Vol. 668 of *Springer Notes in Mathematics,* edited by N. G. Markley, J. C. Martin, and W. Perrizo (Springer-Verlag, Berlin, 1977), p. 48; P. Berge, Y. Pomeau, and C. Vidal, *L'ordre dans le chaos* (Hermann, Paris, 1984).

[23]P. Bergé and M. Dubois, in *Le Chaos,* edited by P. Bergé (CEA, Paris, 1989), Chap. I.

[24]D. Hennequin, D. Dangoisse, M. Lefranc, A. Bekkali, and P. Glorieux (unpublished).

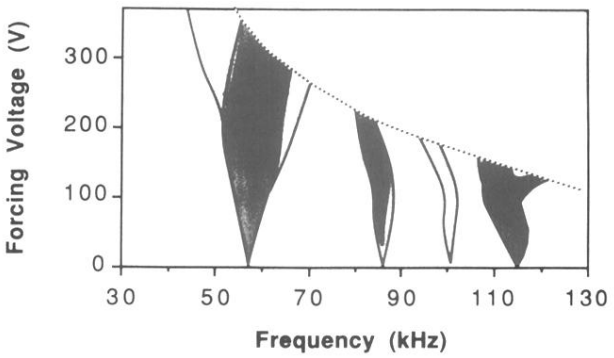

FIG. 3. Evolution of the dynamical regimes of the periodically driven LSA as a function of the frequency and the amplitude of the external driving. The free LSA was operating in the conditions of the star in Fig. 1. In these conditions, the efficiency of the modulation and the amplifier saturation did not allow the modulation rate to increase enough to observe the intersection between the tongues. The white regions correspond to nonperiodic regimes, which may be either chaotic or quasiperiodic. The shaded zones correspond to locked regimes. In the bright gray region, the period of the driven system is the same as that of the forcing one. The middle (dark) gray corresponds to a period doubling (period quadrupling) of the response compared to the forcing. The white zone over the dotted line corresponds to a region that could not be explored because of the bandwidth limitation of the amplifier used in this experiment.

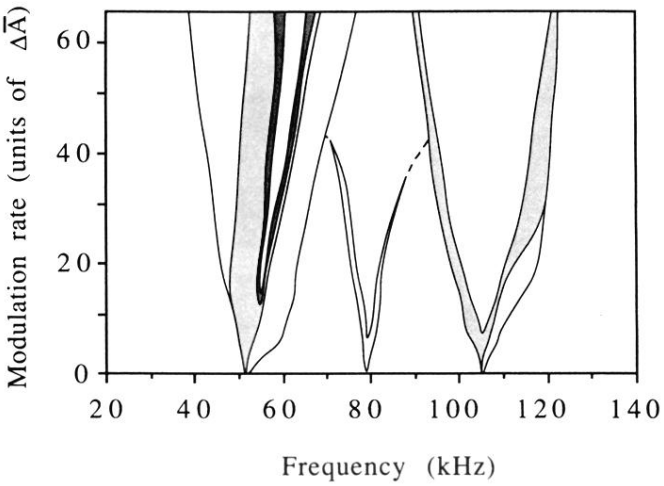

FIG. 5. Calculated phase diagram as a function of the driving frequency. The parameters used are those of Table I. The frequency of the free system is 53 kHz. For the sake of simplicity, only the three first main tongues have been represented: they are respectively associated with the winding numbers 1 (53 kHz), 1/2 (106 kHz), and 2/3 (89 kHz). The 1/3 tongue is outside the limits of the figure. The dashed lines of the 2/3 tongue have been represented to clarify the figure, but the corresponding limit has not been accurately checked. The white regions correspond to nonperiodic regimes, identified as chaos inside the tongues. On the contrary, outside the tongues, these regimes may be either chaotic or quasiperiodic. The colored zones correspond to locked regimes. In the bright gray region, the period of the driven system is the same as that of the forcing one. The middle (dark) gray corresponds to a period doubling (period quadrupling) of the response compared to the forcing. The other components of the period-doubling cascade are too narrow and so not represented here.